Pramana – J. Phys. (2019) 92:73
https://doi.org/10.1007/s12043-019-1732-4

Magnetohydrodynamic mixed convective flow of an upper convected Maxwell fluid through variably permeable dilating channel with Soret effect

K PRAVIN KASHYAP, ODELU OJJELA* and SAMIR KUMAR DAS

Department of Applied Mathematics, Defence Institute of Advanced Technology (Deemed University), Pune 411 025, India
*Corresponding author. E-mail: odelu@diat.ac.in, odelu3@yahoo.co.in

MS received 4 July 2018; revised 4 September 2018; accepted 4 October 2018; published online 9 March 2019

Abstract. The effects of Soret and variable porosity on an unsteady magnetohydrodynamic flow of an upper convected Maxwell fluid through an expanding or contracting channel are explored in this article. The temperature and concentration at the walls are maintained at different values. The gravitational forces arising from temperature and concentration gradients are also considered. The behaviour of velocity components, skin friction, temperature and concentration with respect to various non-dimensional parameters has been numerically computed by using an efficient shooting method. Newtonian case has been studied using the current algorithm and the present results are compared with earlier literature. At the boundaries, the heat and mass transfer rates are studied using local Nusselt and Sherwood numbers. The results show that both the variable permeability and wall expansion have dominant effects on skin friction at the plates. The Prandtl and Soret numbers have dominating effect on mass transfer when compared with variable permeable parameter.

Keywords. Upper convected Maxwell fluid; expanding or contracting channel; variable permeability; Soret effect; mixed convection; shooting method.

PACS Nos 47.65.Gx; 47.60.Dx; 44.27.+g; 44.30.+v

1. Introduction

Viscoelastic fluids have immense importance in chemical and biological industrial processes which have applications in the flow of body fluids, dilute polymer solutions like polyethylene oxide or polyacrylamide and manufacturing of food materials. Oldroyd [1] developed a systematic framework for the theoretical formulations of viscoelastic fluids. Formulation of a single constitutive equation which accounts for different physical effects is very difficult. Hence, several models, for e.g. [2–8] have been developed by formulating a stress differential equation with Oldroyd, Gordon–Schowalter, upper and lower convected derivatives. Among these models, upper convected Maxwell (UCM) model is the most popular due its practical applicability and less mathematical complications [9]. UCM model is a model in the nonlinear flow regime which accounts for frame invariance and leads to relatively less convergence and stability related issues. But, this model can only explain succinct amalgamation of viscous fluids and Hooke's law for elastic solids, but not the complex effects of other viscoelastic formulations. A vast literature [10–14] on UCM fluid above the stretching sheet has been developed by the researchers where they have analysed heat and mass transfer properties for various effects. The seepage of UCM fluids through porous channels is analogous to the unsteady squeeze film flow with separable extensional effects which has various applications like lubrication and viscometry. Choi *et al* [15] extended the Berman [16] problem with UCM fluid by using the Stokes function to investigate the effect of Deborah number on the velocity profiles, pressure gradient, normal and shear stresses. He observed that there is a flattening effect of longitudinal velocity around the middle line and a boundary layer is established around the porous wall. He also observed that when Deborah number increases, the axial velocity of the UCM fluid at the centreline decreases due to viscoelastic effect. Hayat and Abbas [17] considered the 2D steady flow of a UCM fluid through a

porous channel in the presence of chemical reaction and studied the influence of chemical reaction parameter, Reynolds, Deborah and Schimidt numbers on the concentration and velocity fields. The presence of magnetic field in the channel electrical conducting nature shows a huge deviation due to the electric conducting nature of the fluid. Magnetohydrodynamic flows have great importance in power generation and other industrial processes. Hence, Nityadevi *et al* [18], Sandeep and Gnaneswara Reddy [19] have studied the magnetic effects in viscous formulations. The study has been extended to non-Newtonian fluids like Carreau fluids [20,21] and they have explored the combined effects of magnetic and rheological properties. Abbasi *et al* [22] investigated the effect of Reynolds, Hartman and Deborah numbers on velocity distributions by considering the porous slip condition at the upper plate.

The viscoelastic flows in porous media have applications in petroleum and chemical industries where both species diffusion and viscoelastic flow have their impact on the heat and mass transfer. Packed bed reactors, separation systems, polymer processing, filtration systems, foodstuffs and petroleum displacement in reservoirs are some of the important examples of such flows. Wissler [23] explained the development of elongation stresses during the flow of a viscoelastic fluid through a Darcian medium. He noticed that the presence of the porous medium reduces the mobility of the fluid. Later, James and McLaren [24] studied the flow of dilute solutions of viscoelastic fluids (which consist of polyethylene oxide) through layers of packed beads and presented an experimental study of pressure drops and flow rate, which shows that the viscoelasticity is prevalent in moderate flows, whereas at higher flow rates the viscoelastic effect is reduced by the extensional stresses. Both experimental and theoretical studies [25–29] have suggested different models incorporating modified Darcy law, volume averaging techniques over the capillary tubes to investigate the effect of porous media on the flow of viscoelastic fluids. De Haro *et al* [30] implemented a volume averaging technique to study the influence of time-dependent permeability on the Maxwell fluid flow through a rigid porous medium. Bég and Makinde [31] assumed a Darcy model by relating drop in the pressure along the porous medium with a linearly changing drag force and investigated the effect of permeability and viscoelasticity on the velocity and concentration distributions using Runge–Kutta sixth-order method.

Expanding or contracting channels have gained their importance due to the applications in chemical and biological processes. The early study of viscous fluid flows through permeable channels started with Berman [16] who has studied the effect of constant suction and injection through a uniformly porous channel using a mathematical model with analytical solutions by assuming a Stokes stream function and suitable similarity transformations. Understanding the importance of seepage across permeable walls, several models [32–40] have been developed for deformable channels as applications to mass transfer between air tissue and blood, biological filter functions like the lungs and kidneys, responsiveness of endothelial cells, characterisation of atherosclerosis, flow dynamics in predicting pulsatory flow attributes, dialysis in artificial kidneys and peristaltic transport. Majdalini *et al* [41] have constituted a model where the fluid propagation is induced by contractions of two thin plates causing a downstream convection of the fluid in the channel. This has applications for the mass transfer in biological organisms inside a dilating container with permeable walls, which produce the effect of physiological pump. The model consists of a uniformly expanding or contracting channel with a laminar incompressible flow of a Newtonian fluid between two weakly permeable surfaces. Majdalini *et al* [41] and Majdalani and Zhou [42] have obtained the solution using suitable similarity transformations and thus obtained the Proudman–Johnson equation which can be reduced to Berman's equations by taking the zero wall expansion. Several researchers have extended this work with the help of similarity transformations and studied the effect of wall dilation parameters on the flow field variables for small permeation Reynolds by using both analytical and numerical procedures [43–45]. This work has been further extended for non-Newtonian fluids like couple stress, micropolar, viscoelastic and Sisko fluids [46–49] in deformable channels to study the heat and mass transfer characteristics of the fluid.

However, the aforementioned studies of the UCM fluid flow considered permeable channels with fixed plates. In the current article, we have developed a model with upper convected Maxwell fluid in an expanding or contracting porous channel filled with variably permeable porous medium. By following Majdalni *et al* [41] and extending the study to temperature and concentration by maintaining the walls at different temperatures and concentrations, assuming the effects of mixed convection and Soret, the dependence of skin friction, local Nusselt and Sherwood numbers on wall expansion, variable permeability, Prandtl and Soret parameters have been explored in detail through graphs. The effect of mixed convection on temperature and concentration is studied for various Eckart and Sherwood numbers. The results are obtained by using the shooting method and a comparison between the Newtonian case and earlier literature is presented in table 1.

Table 1. Comparison values of axial velocity in the case of Newtonian fluid at Re = 5 and $\alpha = -0.5$.

λ	Majdalani *et al* [41]	Boutros *et al* [43]	Asghar *et al* [45]	Present
0	1.535426	1.515104	1.492595	1.4926
0.05	1.531279	1.511345	1.489084	1.4891
0.1	1.518837	1.500051	1.478534	1.4785
0.15	1.498104	1.481177	1.460893	1.4609
0.2	1.469083	1.454653	1.436081	1.4361
0.25	1.431787	1.420383	1.403991	1.4040
0.3	1.386238	1.378261	1.364499	1.3645
0.35	1.332474	1.328174	1.317471	1.3175
0.4	1.27056	1.270018	1.262772	1.2628
0.45	1.20059	1.203708	1.200279	1.2003
0.5	1.122702	1.1292	1.129885	1.1299
0.55	1.03709	1.046507	1.051513	1.0515
0.6	0.944014	0.955722	0.965127	0.9651
0.65	0.843823	0.857047	0.870736	0.8707
0.7	0.736968	0.750818	0.768404	0.7684
0.75	0.634023	0.637541	0.658261	0.6583
0.8	0.505712	0.517928	0.540502	0.5405
0.85	0.38553	0.392938	0.415401	0.4154
0.9	0.259708	0.263822	0.283311	0.2833
0.95	0.131204	0.132178	0.144668	0.1447
1	0	0	0	0.0000

2. Formulation of the problem

In this model, we deal with an unsteady flow of UCM fluid through an expanding or contracting porous semi-infinite channel, the plates are placed at $y = -a$ and $y = a$. One of the channel ends is bounded by a stretching sheet or membrane which stretches or contracts as the distance between the plates, $a(t)$, changes with time and the wall expansion rate, i.e. $\dot{a}(t)$ is constant. For the axial velocity, no-slip condition is assumed at the boundaries. It is assumed that the fluid is constantly sucked or injected from the plate with a velocity V_1, the temperature and concentration at the plates are constantly maintained at T_1, C_1 and T_2, C_2, where T_1 is temperature at the lower plate, C_1 is the concentration at the lower plate, T_2 is the temperature at the upper plate and C_2 is the concentration at the upper plate. The governing equations are given by eqs (1)–(6).

$$\nabla \cdot q = 0, \tag{1}$$

$$\frac{\partial \vec{q}}{\partial t} + (\vec{q} \cdot \nabla)\vec{q} = -\nabla P + \nabla \cdot S + \mu \nabla^2 \vec{q} - J \times B - \frac{\mu}{k_1}\vec{q} + \rho g(\beta_T (T - T_1) + \beta_C (C - C_1)), \tag{2}$$

$$\rho c \left[\frac{\partial T}{\partial t} + (\vec{q} \cdot \nabla)T\right] = k\nabla^2 T + \frac{J^2}{\sigma}, \tag{3}$$

$$\frac{\partial C}{\partial t} + (\vec{q} \cdot \nabla)C = D\nabla^2 C + \frac{DK_T}{T_m}\nabla^2 T, \tag{4}$$

where

$$k_1 = k_0(1 + k_p e^{\lambda}) \tag{5}$$

$$S + \beta\left(\frac{\mathrm{d}S}{\mathrm{d}t} + \vec{q} \cdot \nabla S - (\nabla \vec{q})^T \cdot S - S \cdot \nabla \vec{q}\right) = \mu\left(\nabla \vec{q} + (\nabla \vec{q})^T\right). \tag{6}$$

Here λ is the dimensionless y coordinate. It is assumed that the dependence of permeability across the channel is governed by eq. (5). S denotes the extra stress tensor which is governed by the partial differential equation (PDE) (6) with an upper convected derivative and relaxation parameter β. The first two terms in (6) represent the time and material derivatives while the other two represent the deformation of the fluid. Physically, these terms represent the rotation, convection and stretching of the fluid motion, such that frame invariance is satisfied. The x and y-axes are chosen along and perpendicular to the axial flow direction, the magnetic field of constant magnitude is applied in the z-direction as shown in figure 1. The Darcy resistive force is considered by assuming a variation in permeability along the y-axis and time (function of λ). The gravitational forces arising from temperature and concentration gradients are characterised by the thermal and solutal expansion coefficients (β_T and β_C). σ is the electrical conductivity of the fluid, J is the current density and the term $J \times B$ is the Lorentz force acting on the fluid. The Joule heating due to the Lorentz forces is also considered in the energy equation. The change in the concentration of the fluid

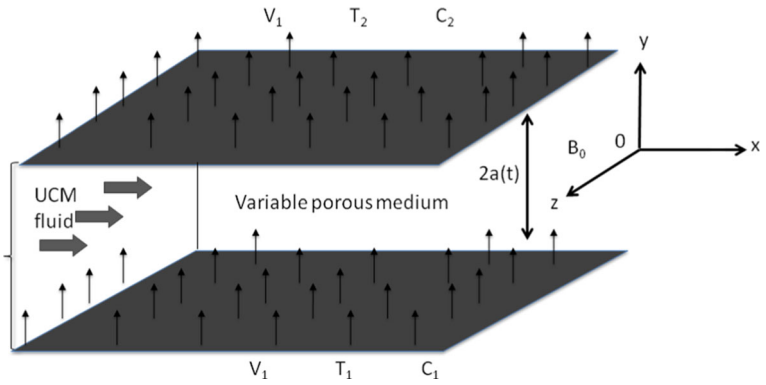

Figure 1. The schematic diagram of UCM fluid flow through expanding/contracting plates.

due to temperature differences is studied by considering the Soret effect. With all these assumptions, the governing equations in the Cartesian coordinate system can be represented by eqs (7)–(11).

$$\frac{\partial u}{\partial x}+\frac{\partial v}{\partial y}=0, \tag{7}$$

$$\rho\left[\frac{\partial u}{\partial t}+u\frac{\partial u}{\partial x}+v\frac{\partial u}{\partial y}+\beta\left(u^2\frac{\partial^2 u}{\partial x^2}+v^2\frac{\partial^2 u}{\partial y^2}+2uv\frac{\partial^2 u}{\partial x\partial y}\right)\right]=-\frac{\partial P}{\partial x}+\mu\nabla^2 u-\sigma B_0^2 u+\rho g\beta_T(T-T_1)+\rho g\beta_C(C-C_1)-\frac{\mu}{k_1}u, \tag{8}$$

$$\rho\left[\frac{\partial v}{\partial t}+u\frac{\partial v}{\partial x}+v\frac{\partial v}{\partial y}+\beta\left(u^2\frac{\partial^2 v}{\partial x^2}+v^2\frac{\partial^2 v}{\partial y^2}+2uv\frac{\partial^2 v}{\partial x\partial y}\right)\right]=-\frac{\partial P}{\partial y}+\mu\nabla^2 v-\sigma B_0^2 v-\frac{\mu}{k_1}v, \tag{9}$$

$$\rho c\left[\frac{\partial T}{\partial t}+u\frac{\partial T}{\partial x}+v\frac{\partial T}{\partial y}\right]=k\left(\frac{\partial^2 T}{\partial x^2}+\frac{\partial^2 T}{\partial y^2}\right)+\sigma B_0^2(u^2+v^2), \tag{10}$$

$$\frac{\partial C}{\partial t}+u\frac{\partial C}{\partial x}+v\frac{\partial C}{\partial y}=D\left(\frac{\partial^2 C}{\partial x^2}+\frac{\partial^2 C}{\partial y^2}\right)+\frac{D_1 K_T}{T_{\mathrm{m}}}\left(\frac{\partial^2 T}{\partial^2 x}+\frac{\partial^2 T}{\partial^2 y}\right), \tag{11}$$

where ρ is the density of the fluid, P is pressure, μ is the viscosity of the fluid, C is the specific heat at constant temperature, k is the thermal conductivity, D is the diffusivity coefficient, T_{m} is the mean temperature and B_0 is the magnetic flux density. The boundary conditions at the lower and upper plates are as follows:

$$\begin{aligned}&u(x,y,t)=0,\quad v(x,y,t)=V_1,\\&T(x,y,t)=T_1,\quad C(x,y,t)=C_1\quad \text{at } y=-a(t),\\&u(x,y,t)=0,\quad v(x,y,t)=-V_1,\\&T(x,y,t)=T_2,\quad C(x,y,t)=C_2\quad \text{at } y=a(t),\end{aligned} \tag{12}$$

where u is the velocity component in the x-direction and v is the velocity component in the y-direction. We assume a similarity solution of the form (13).

$$\begin{aligned}&u(x,\lambda,t)=\frac{vx}{a^2}F'(\lambda,t),\quad v(x,\lambda,t)=-\frac{v}{a}F(\lambda,t)\\&T(x,\lambda)=T_1+\frac{vV_1}{ac}\left(\phi_1(\lambda)+\frac{x^2}{a^2}\phi_2(\lambda)\right)\\&C(x,\lambda)=C_1+\frac{\dot{n}_A}{av}\left(g_1(\lambda)+\frac{x^2}{a^2}g_2(\lambda)\right).\end{aligned} \tag{13}$$

Here $\dot{n}_A$ is the mass transfer rate. Now, a similarity solution in time and space is derived for constant α's which are specified by the initial value

$$\alpha=\frac{a\dot{a}}{\nu}=\frac{a_0\dot{a}_0}{\nu},$$

where a_0, $\dot{a}_0$ are the initial distance and wall expansion ratios and ν is the kinematic viscosity. By following Asghar *et al* [45], instead of λ and t, the function F is redefined to be a function of λ and $\alpha(t)$. By assuming α to be constant or quasiconstant in time, we have the condition $F_{\lambda t}=0$. The relation between F and f is given by $F(\lambda)=\mathrm{Re}\,f(\lambda)$. The velocity components, temperature and concentration are substituted in eqs (7)–(11) which transform PDE into nonlinear ordinary differential equations (ODEs). The non-dimensional form of the differential equations is given by eqs (14)–(18).

$$\begin{aligned}&f^{iv}(1-\mathrm{WiRe}\,f^2)\\&=-\alpha(\lambda f'''+3f'')\\&\quad+\mathrm{Re}(f'f''-ff''')-2\mathrm{WiRe}((f')^2f''\\&\quad+f(f'')^2)+\mathrm{Ha}^2f''-\frac{\mathrm{EcGr}}{\xi}(\phi_1'+\xi^2\phi_2')\end{aligned}$$

$$-\frac{\mathrm{ShGc}}{\xi}(g_1' + \xi^2 g_2') + D^{-1}\left(\frac{(1+k_p\mathrm{e}^{\lambda})f'' - k_p e^{\lambda} f'}{(1+k_p\mathrm{e}^{\lambda})^2}\right) \quad (14)$$

$$\phi_1'' = -\alpha\,\mathrm{Pr}(\phi_1 + \lambda\phi_1') - \mathrm{Re}\,\mathrm{Pr}(f\phi_1') - \mathrm{Ha}^2\mathrm{Re}\,\mathrm{Pr}(f^2) - 2\phi_2 \quad (15)$$

$$\phi_2'' = -\alpha\,\mathrm{Pr}(\phi_2 + \lambda\phi_2') + \mathrm{Re}\,\mathrm{Pr}(f'\phi_2 - f\phi_2') - \mathrm{Ha}^2\mathrm{Re}\,\mathrm{Pr}(f')^2 \quad (16)$$

$$g_1'' = -\alpha\mathrm{Sc}(g_1 + \lambda g_1') - \mathrm{ReSc}\,f g_1' - \mathrm{SrSc}(\phi_1'' + 2\phi_2) - 2g_2 \quad (17)$$

$$g_2'' = -\alpha\mathrm{Sc}(g_1 + \lambda g_1') + \mathrm{ReSc}(2f'g_2 - fg_2') - \mathrm{SrSc}\phi_2''. \quad (18)$$

The boundary conditions (19) on $f(\lambda)$, $\phi_1(\lambda)$, $\phi_2(\lambda)$, $g_1(\lambda)$ and $g_2(\lambda)$ represent the velocities, temperature and concentration at the boundaries.

$$\begin{aligned} &f(-1) = 0, \quad f'(-1) = 0,\\ &\phi_1(-1) = 0, \quad \phi_2(-1) = 0,\\ &g_1(-1) = 0, \quad g_2(-1) = 0\\ &f(1) = -1, \quad f'(1) = 0,\\ &\phi_1(1) = 1/\mathrm{Ec}, \quad \phi_2(1) = 0,\\ &g_1(1) = 1/\mathrm{Sh}, \quad g_2(1) = 0. \end{aligned} \quad (19)$$

The prime in the above equations denotes the differentiation with respect to λ, where $\lambda = y/a$, $\alpha = a\dot{a}/\nu$ is the non-dimensional wall expansion ratio, $\zeta = x/a$, $\mathrm{Re} = \rho V_1 a/\mu$ is the Reynolds number, $Wi = \beta V_1/a$, $\mathrm{Ha}^2 = \sigma B_0^2 a^2/\mu$ is the Hartmann number, $\mathrm{Ec} = \mu V_1/\rho a c(T_2 - T_1)$ is the Eckart number, $\mathrm{Gr} = \rho g \beta_T (T_2 - T_1)a^3/\nu^2$, $\mathrm{Gc} = \rho g \beta_C (C_2 - C_1)a^3/\nu^2$ is the solutal Grashoff number, D^{-1} is the inverse Darcy parameter, $\mathrm{Sh} = \dot{n}_A/a\nu(C_2 - C_1)$ is the Sherwood number, $\mathrm{Pr} = \mu c/k$ is the Prandtl number, $\mathrm{Sc} = \nu/D$ is the Schimdt number, Soret number $\mathrm{Sr} = DK_T\nu V_1/cT_{\mathrm{m}}\dot{n}_A$ where T_{m} is the mean temperature and K_T is the Soret temperature.

3. Solution procedure

Finding an analytical solution to this highly nonlinear system is very difficult which leaves the numerical solution as the easy way to understand the properties of the current problem. The nonlinear ODEs (15)–(19) are reduced to a first-order system of differential equations. The boundary values problem (BVP) is solved in two steps, first being an initial value problem (IVP) and the second one is a nonlinear algebraic system. The IVP is integrated using the R–K fourth-order method by using the initial value by assuming slopes which results in a nonlinear algebraic system. The algebraic system is solved by using Newton–Raphson method and the values of initial slopes are found such that the boundary conditions are satisfied. It is to be noted that the choice of initial slopes plays a major role in obtaining the solution of the problem. The results for the axial velocity of the Newtonian fluid flow through an expanding or contracting channel are compared with [34,36,38] using the shooting method and the results are presented in table 1.

4. Results and discussion

The properties of the physical variables between the channel are studied with respect to λ for an arbitrary ξ. The effects of wall expansion parameter and variable permeability parameter on the non-dimensional flow field variables T^*, C^*, C_f^*, Sh^* and Nu^* between the channel are studied in the domain $[-1, 1]$. The dependence of the flow field variables on non-dimensional variables is studied by varying the parameter from 0 to 7. These quantities $U^*(f(\lambda))$, $V^*(f'(\lambda))$, T^*, C^*, C_f^*, Sh^* and Nu^* are non-dimensional quantities defined as follows:

$$T^* = \phi_1(\lambda) + \xi^2\phi_2(\lambda); \quad C^* = g_1(\lambda) + \xi^2 g_2(\lambda);$$
$$C_f^* = f''(\lambda); \quad \mathrm{Nu}^* = -\frac{\partial T^*}{\partial y}; \quad \mathrm{Sh}^* = -\frac{\partial C^*}{\partial y}$$

The effect of variable permeable parameter on the axial and radial velocity profiles in an expanding channel is depicted in figure 2. We can clearly see from eq. (5) that the permeability of the porous medium increases exponentially towards the end of the channel. This variation is clearly visible in the axial velocity profiles where we observe the peak velocities to be increasing with variable permeability parameter. It is also noticed that the axial velocity profiles tend to decrease towards the walls. The radial velocity of the UCM fluid decreases till the middle of the channel and shows an opposite behaviour towards the upper plate.

The effects of expanding, contracting and fixed boundaries on the Prandtl, Soret and variable permeability parameters are shown in figures 3–5. The thick line shows the effect of contraction on the variation of k_p, Pr and Sr on C_f^*, Sh^* and Nu^*. The dashed and dotted lines represent fixed and expanding channels respectively. It can be deduced from the figures that the negative expansion parameter, i.e. contraction increases the skin friction at the lower plate, but it reduces the value of C_f^* at the upper plate. The local Nusslet number which corresponds to the heat transfer rate at the boundaries is enhanced by wall contraction at the lower plate whereas it reduces Nu^* at the upper plates. So, by decreasing the wall expansion ratio, the heat transfer rate at the lower plate can be enhanced. The local Sherwood number at

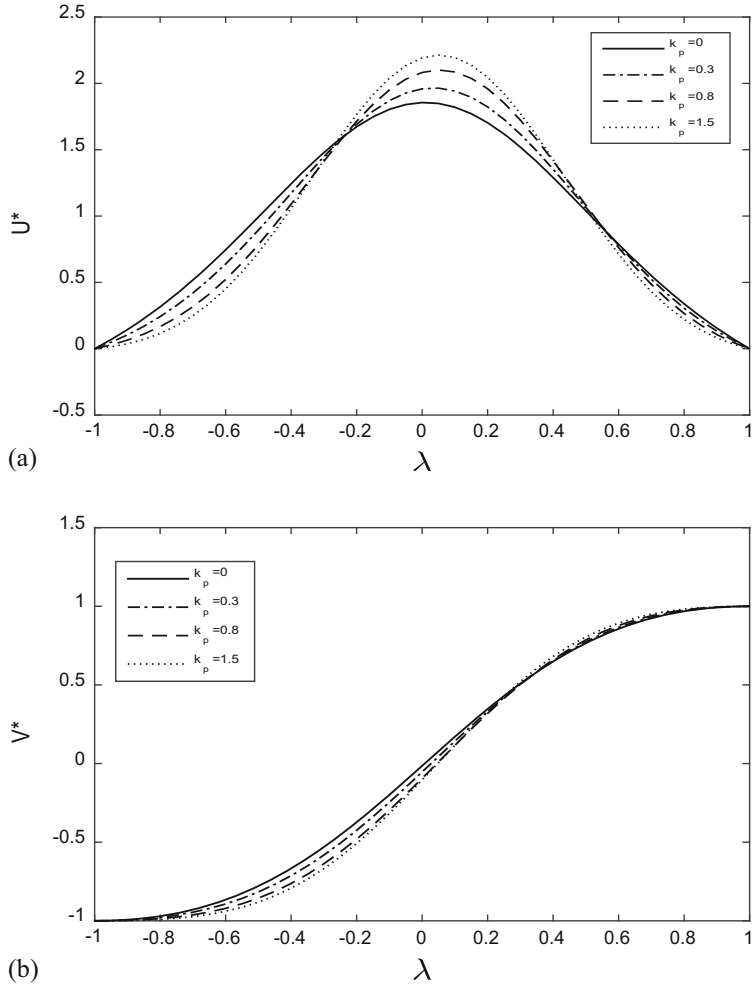

Figure 2. Effect of variable permeable parameter on (**a**) axial and (**b**) radial velocity components at Re = 0.2, $D^{-1} = 10$, Wi = 0.03, Gr = 0.04, Gc = 0.04, Sc = 0.4, ξ = 0.6325, Sh = 1, Ha = 0.5, α = 6, Pr = 0.71, Sr = 0.2 and Ec = 0.1.

the upper plate is also enhanced by the wall expansion parameter and it reduces the mass transfer rate at the lower plate.

Figure 3 shows the effect of variable permeability parameter on the skin friction, local Nusselt and Sherwood numbers at the plates. It can be observed that high permeability results in a gradual increment of skin friction (C_f^*) at the upper plate and the opposite at the lower plate. The local Nusselt number at the lower plate gains a maximum value around $k_p = 1$ and then decreases, and this is due to the increment of permeability in eq. (5). A slight decrement in Nu* at the upper plate is observed for k_p in [0,1] and then it increases. The local Sherwood number profile follows a trend similar to that of the local Nusslet number.

The effect of variation of Prandtl number on Nu* and Sh* at the boundaries can be observed in figure 4. The numerical experiment is carried by increasing the Prandtl number, i.e. momentum to thermal diffusivity ratio from 1 to 7 in order to study the heat and mass transfer properties at the walls. The local Nusslet number is also found to be increasing for increasing Pr at the boundaries. As the Prandtl number is the ratio of viscous and thermal diffusion rates, the increment of Prandtl number refers to the dominance of viscous diffusivity and it has a dominant effect in the expanding channel due to its wall motion. The Sh* values are found to be decreasing for increasing Pr values at both upper and lower plates.

The dependence of the local Sherwood number on the Soret number is depicted in figure 5. The Soret effect is prevalent in systems where the temperature gradients are big enough to cause concentration changes in the system and it is generally studied with Soret parameter (Sr). The Soret parameter enhances the species concentration due to temperature gradients, thus increasing Sr has a direct relation to the local Sherwood number. It can be clearly seen that Sh* decreases with Sr at the upper and lower plates.

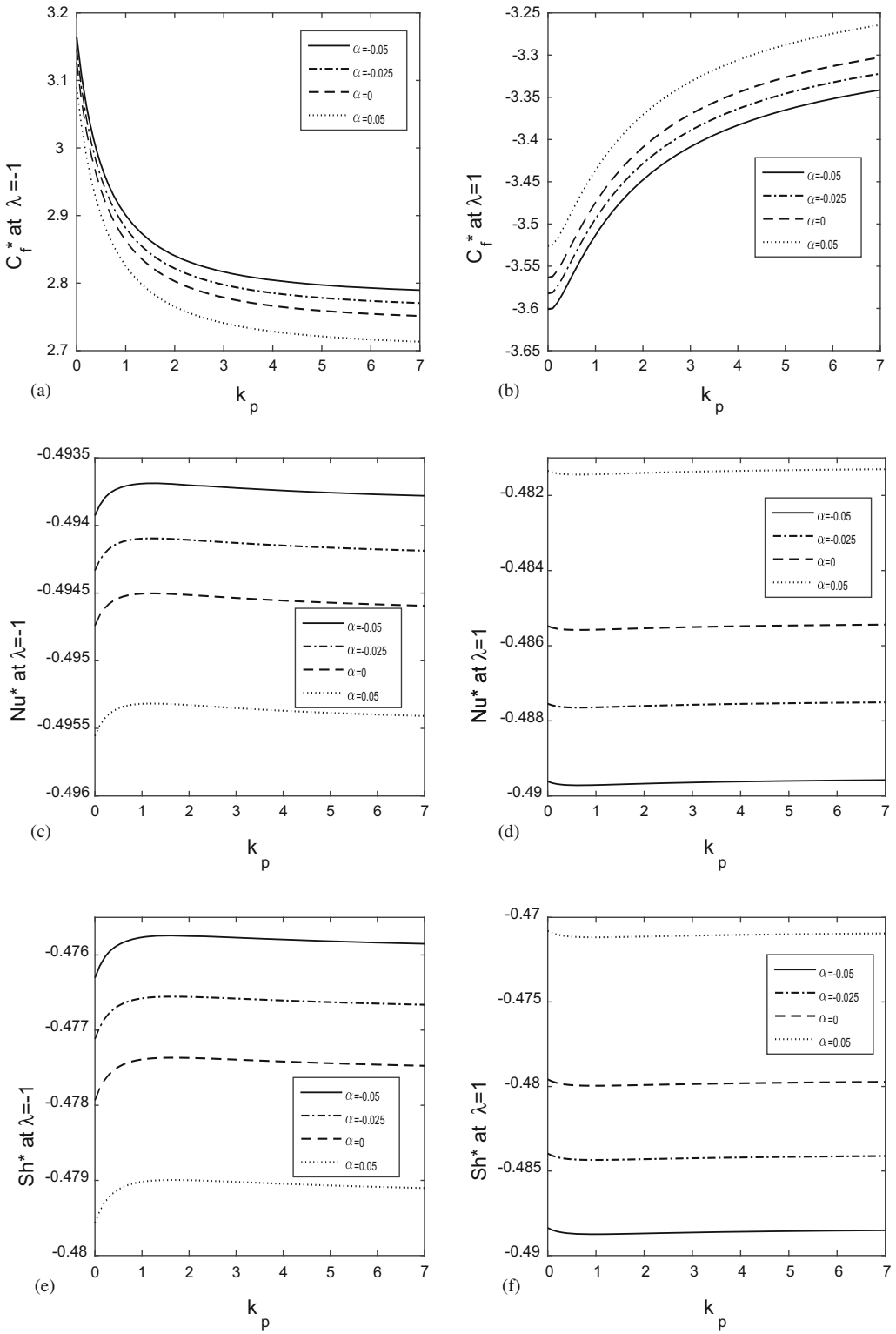

Figure 3. Effect of contracting, fixed and expanding channel on C_f^*, Sh* and Nu* at lower and upper plates with respect to k_p when Re = 0.5, $D^{-1} = 2$, Wi = 0.1, Gr = 0.25, Gc = 0.25, Sc = 0.22, ξ = 0.6325, Sh = 1, Ha = 0.2, Pr = 0.71, Sr = 0.1 and Ec = 1.

However, it can be observed that the C_f^* values are greatly influenced by k_p when compared to Pr and Sr. The variation of k_p increases the permeability and thus reduces the resisting force due to the Darcy's law. The effect of Pr on the heat transfer coefficient is dominant when compared to k_p and Sr.

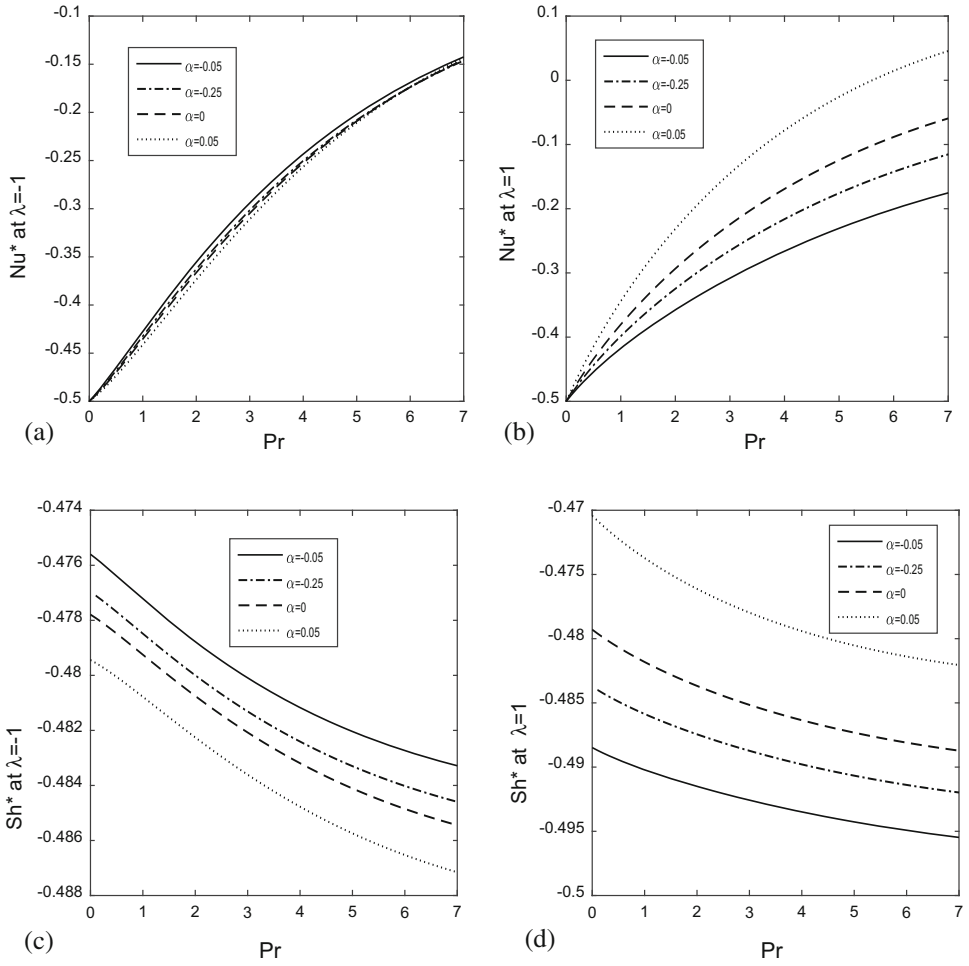

Figure 4. Effect of contracting, fixed and expanding channel on Nu* and Sh* at lower and upper plates with respect to Pr when Re = 0.5, $D^{-1} = 2$, Wi = 0.1, Gr = 0.25, Gc = 0.25, Sc = 0.22, ξ = 0.6325, Sh = 1, Ha = 0.2, α = 0.05, $k_p = 2$, Sr = 0.1 and Ec = 1.

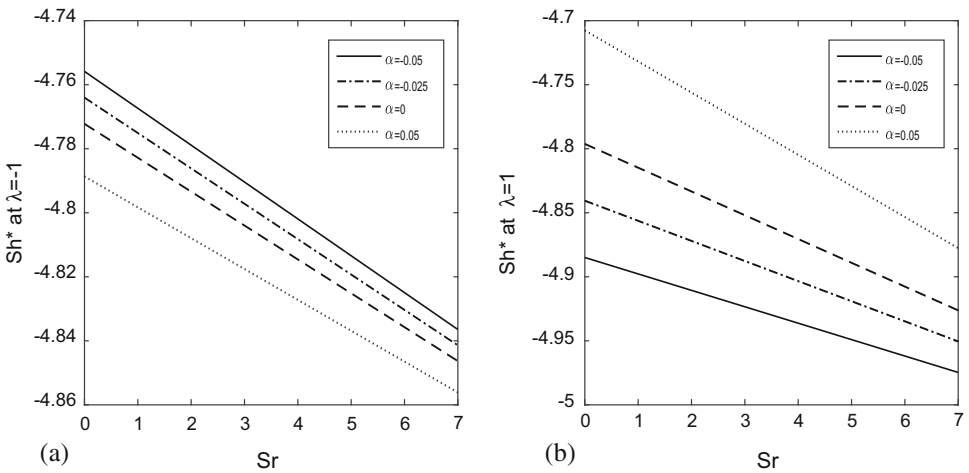

Figure 5. Effect of contracting, fixed and expanding channel on Sh* at (**a**) lower and (**b**) upper plates with respect to Sr when Re = 0.5, $D^{-1} = 2$, Wi = 0.1, Gr = 0.25, Gc = 0.25, Sc = 0.22, ξ = 0.6325, Sh = 1, Ha = 0.2, α = 0.05, $k_p = 2$, Pr = 0.71 and Ec = 1.

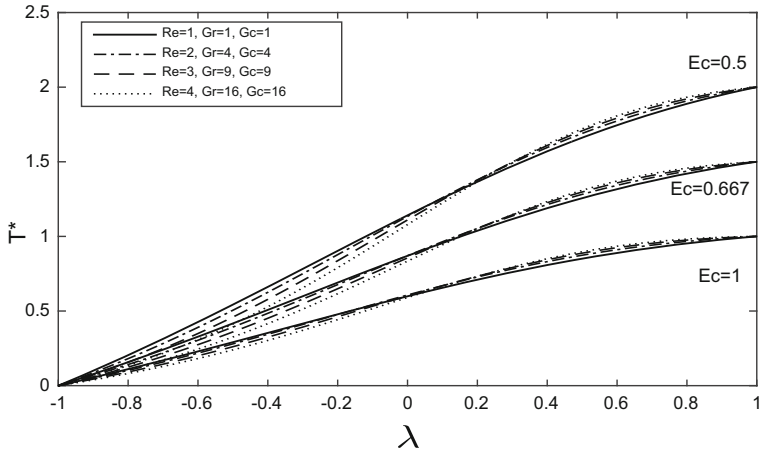

Figure 6. Effect of mixed convection and Eckart number on temperature profiles when $D^{-1} = 2$, Wi $= 0.1$, Sc $= 0.5$, $\xi = 0.6325$, Sh $= 1$, Ha $= 0.4$, $\alpha = 0.5$, $k_p = 2$, Pr $= 0.4$ and Sr $= 1$.

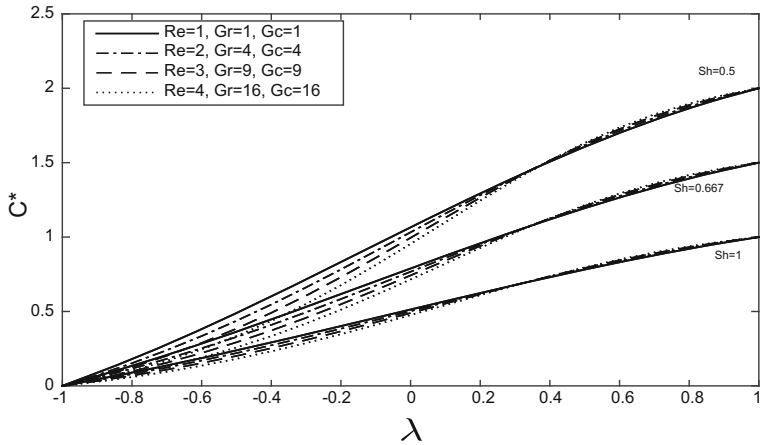

Figure 7. Effect of mixed convection and Sherwood number on concentration profiles when $D^{-1} = 2$, Wi $= 0.1$, Sc $= 0.22$, $\xi = 0.6325$, Ha $= 0.4$, $\alpha = 0.5$, $k_p = 2$, Pr $= 0.4$, Sr $= 1$ and Ec $= 1$.

The effect of mixed convection on temperature and concentration is presented in figures 6 and 7. As there are temperature and concentration gradients in the system, it is quite natural that convective forces arise in the system. The effect of mixed convection is studied by varying the Reynolds number, thermal and solutal Grashoff numbers such that they follow the relation $\mathrm{Gr}/\mathrm{Re}^2 = \mathrm{Gc}/\mathrm{Re}^2 = 1$. It is very clear that the Eckart and Sherwood numbers have a clear effect on T^* and C^* at the upper plate. The temperature in the channel increases with Eckart number while the species concentration increases for increasing Sherwood number. As thermal and solute buoyancy forces increase, the temperature and concentration increase till the middle of the channel and then decreases towards the upper plate.

5. Conclusions

The effect of wall expansion, variable permeability and other non-dimensional parameters on skin friction, local Nusselt and Sherwood numbers has been numerically investigated for an unsteady MHD flow of a UCM fluid through a variably permeable porous channel. The conclusions are listed as follows:

1. The wall expansion enhances the skin friction, heat and mass transfer at the upper wall and reduces the same at the lower wall.
2. The variable permeability has dominating effect on the skin friction when compared to the Prandtl and Soret numbers.
3. Heat transfer at the plates is greatly influenced by the Prandtl number when compared to variable permeability parameter.
4. Both Prandtl and Soret numbers have a deep effect on mass transfer and they both have a decreasing effect on Sh*.
5. Mixed convection on temperature and concentration is studied with increasing Reynolds number for various Eckart and Sherwood numbers.

The above results can have possible applications in polymers, lubrication and other biological processes.

Acknowledgements

The authors are thankful to the Vice Chancellor of Defence Institute of Advanced Technology (Deemed University) for his support in the current research. One of the authors (KPK) is grateful to the University Grants Commission, Government of India for providing Senior Research Fellowship (F.2-18/2012(SA-I)).

References

[1] J G Oldroyd, *Proc. R. Soc. London A* **200**, 523 (1950)
[2] C Ruan and J Ouyang, *Chin. J. Chem. Eng.* **18**(**2**), 177 (2010)
[3] S Dhinakaran, A M Afonso, M A Alves and F T Pinho, *J. Colloid Interface Sci.* **344**(**2**), 513 (2010)
[4] K Satish, V Průša and K R Rajagopal, *Int. J. Non-Linear Mech.* **46**(**6**), 819 (2011)
[5] T Hayat and N Ali, *Physica A* **370**(**2**), 225 (2006)
[6] O Prakash, D Kumar and Y K Dwivedi, *Pramana – J. Phys.* **79**(**6**), 1457 (2012)
[7] A A Afify and M A El-Aziz, *Pramana – J. Phys.* **88**(**2**): 31 (2017)
[8] N Sandeep and M Gnaneswara Reddy, *Eur. Phys. J. Plus* **132**(**3**), 147 (2017)
[9] S Middleman, *Fundamentals of polymer processing* (McGraw-Hill College, 1977)
[10] A Alizadeh-Pahlavan and K Sadeghy, *Commun. Nonlinear Sci. Numer. Simulat.* **14**(**4**), 1355 (2009)
[11] T Hayat and M Awais, *Int. J. Numer. Methods Fluids* **66**(**7**), 875 (2011)
[12] M Nandeppanavar Mahantesh, K Vajravelu and M Subhas Abel, *Commun. Nonlinear Sci. Numer. Simulat.* **16**(**9**), 3578 (2011)
[13] M Jayachandra Babu and N Sandeep, *J. Mol. Liq.* **232**, 27 (2017)
[14] S Mukhopadhyay, *Chin. Phys. Lett.* **29**(**5**), 054703 (2012)
[15] J J Choi, Z Rusak and J A Tichy, *J. Non-Newtonian Fluid Mech.* **85**(**2**), 165 (1999)
[16] A S Berman, *J. Appl. Phys.* **24**(**9**), 1232 (1953)
[17] T Hayat and Z Abbas, *Z. Angew. Math. Phys.* **59**(**1**), 124 (2008)
[18] N Nithyadevi, P Gayathri and N Sandeep, *Int. J. Mech. Sci.* **131**, 827 (2017)
[19] N Sandeep and M Gnaneswara Reddy, *J. Mol. Liq.* **225**, 87 (2017)
[20] T Hayat, M Waqas, S A Shehzad and A Alsaedi, *Pramana – J. Phys.* **86**(**1**), 3 (2016)
[21] P M Krishna, N Sandeep and R P Sharma, *Eur. Phys. J. Plus* **132**(**5**), 202 (2017)
[22] M Abbasi, M Khaki, A Rahbari, D D Ganji and I Rahimipetroudi, *J. Braz. Soc. Mech. Sci. Eng.* **38**(**3**), 977 (2016)
[23] E H Wissler, *Ind. Eng. Chem. Fundam.* **10**(**3**), 411 (1971)
[24] D F James and D R McLaren, *J. Fluid Mech.* **70**, 733 (1975)
[25] J A Deiber and W R Schowalter, *AlChE J.* **27**(**6**), 912 (1981)
[26] F Durst, W Haas and W Interthal, *J. Non-Newtonian Fluid Mech.* **22**(**2**), 169 (1987)
[27] K K Talwar and B Khomami, *J. Rheol.* **36**(**7**), 1377 (1992)
[28] W Tan and T Masuoka, *Phys. Fluids* **17**, 23 (2005)
[29] J Savins, *Ind. Eng. Chem.* **61**(**10**), 18 (1969)
[30] M L De Haro, J A P Del Río and S Whitaker, *Transp. Porous Med.* **25**(**2**), 167 (1996)
[31] O A Bég and O D Makinde, *J. Petroleum Sci. Eng.* **76**, 93 (2011)
[32] H N Chang, J S Ha, J K Park, I H Kim and H D Shin, *J. Biomech.* **22**, 1257 (1989)
[33] C F J Dewey, S R Bussolari, M A J Gimbrone and P F Davis, *J. Biomech. Eng.* **103**, 177 (1981)
[34] J M Drazen, R D Kamm and A S Slutsky, *Physiol. Rev.* **64**, 505 (1984)
[35] Y C Fung and C S Yih, *J. Appl. Mech.* **35**, 669 (1968)
[36] M Goto and S Uchida, *Proceedings of the 40th Japan National Congress on Applied Mechanics* (NCTAM-40) (1990) p. 163
[37] M J Levesque and R M Nerem, *J. Biomech. Eng.* **107**, 341 (1985)
[38] S Uchida and H Aoki, *J. Fluid Mech.* **82**, 371 (1977)
[39] C Y Wang, *ASME Trans. J. Appl. Mech.* **38**, 553 (1971)
[40] G Sucharitha, P Lakshminarayana and N Sandeep, *Int. J. Mech. Sci.* **131**, 52 (2017)
[41] J Majdalani, C Zhou and C A Dawson, *J. Biomech.* **35(10)**, 1399 (2002)
[42] J Majdalani and C Zhou, *Zeitschrift für Angewandte Mathematik und Mechanik* **83**, 181 (2003)
[43] Y Z Boutros, M B Abd-el-Malek, N A Badran and H S Hassan, *Appl. Math. Model.* **31**(**6**), 1092 (2007)
[44] S Asghar, M Mushtaq and A Kara, *Appl. Math. Model.* **32**(**12**), 2936 (2008)
[45] S Asghar, M Mushtaq and T Hayat, *Nonlinear Anal. Real World Appl.* **11**(**1**), 555 (2010)
[46] D Srinivasacharya, N Srinivasacharyulu and O Odelu, *Int. Commun. Heat Mass Transfer* **36**(**2**), 180 (2009)
[47] S Xinhui, Z Liancun, C Xuehui, Z Xinxin, C Limei and L Min, *Comput. Methods Biomech. Biomed. Eng.* **17**(**4**), 423 (2014)
[48] X Si, L Zheng, X Zhang, X Si and M Li, *Comput. Methods Biomech. Biomed. Eng.* **17**(**6**), 623 (2014)
[49] Y Wang, T Hayat, N Ali and M Oberlack, *Physica A* **387**(**2–3**), 347 (2008)